



# Radiation-transfer modeling of snow-pack photochemical processes during ALERT 2000

William R. Simpson<sup>a,\*</sup>, Martin D. King<sup>a,1</sup>, Harald J. Beine<sup>b,2</sup>, Richard E. Honrath<sup>b</sup>, Xianliang Zhou<sup>c</sup>

<sup>a</sup>Department of Chemistry, International Arctic Research Center, Geophysical Institute, University of Alaska Fairbanks, Fairbanks, AK 99775-6160, USA

<sup>b</sup>Department of Civil and Environmental Engineering, Michigan Technological University, 1400 Townsend Drive, Houghton, MI 49931, USA

<sup>c</sup>Wadsworth Center/NYSDOH, and School of Public Health/SUNY at Albany, Albany, NY, USA

Received 4 June 2001; received in revised form 4 August 2001; accepted 11 January 2002

## Abstract

The delta-Eddington radiation transfer model is used to calculate actinic fluxes and photolysis rates within the snow pack during the ALERT 2000 field campaign. Actinic fluxes are enhanced within the snow pack due to the high albedo of snow and conversion of direct light to diffuse light. The conversion of direct to diffuse light is highly dependent on the solar zenith angle, as demonstrated by model calculations. The optical properties of Alert snow are modeled as 100  $\mu\text{m}$  radius ice spheres with impurity added to increase the absorption coefficient over that of pure water ice. Using these optical properties, the model achieves good agreement with observations of irradiance within the snow pack. The model is used to calculate the total actinic flux as a function of solar zenith angle and depth for either clear sky or cloudy conditions. The actinic flux is then used to calculate photochemical production of nitrogen oxides from nitrate photolysis assuming that nitrate in snow has the same absorption cross section and quantum yield in snow as in aqueous solution. Assuming all photo-produced nitrogen oxides are released to the gas phase, we derive a maximal flux of nitrogen oxides ( $\text{NO}_x + \text{HONO}$  and possibly other products) from the snow pack. The value of this maximal flux depends critically on the assumed quantum yield for production of  $\text{NO}_2$ , which is unknown in ice. Depending on the assumed quantum yield, the calculated maximal flux varies between values four times smaller than the observed  $\text{NO}_x + \text{HONO}$  flux to five times larger than the  $\text{NO}_x + \text{HONO}$  flux. Therefore, it appears that the calculated flux is in approximate agreement with the observations with a great need for improved understanding of nitrogen photochemistry in snow. © 2002 Elsevier Science Ltd. All rights reserved.

**Keywords:**  $\text{NO}_x$ ; Snow; Nitrate ion; Arctic; Surface fluxes

## 1. Introduction

Recent studies indicate that ultraviolet light drives photochemical processes within the snow pack (Couch

et al., 2000; Honrath et al., 1999, 2000a, b; Hutterli et al., 1999; Jones et al., 1999, 2000; Sumner and Shepson, 1999). One of the goals of the ALERT 2000 campaign was to investigate the chemical fluxes produced by these photochemical processes. Specifically, we were interested in the production of  $\text{NO}_x$  from snow-pack nitrate photolysis. This chemistry is one of the most clearly indicated snow-pack photochemical processes (Hoffman, 1996; Honrath et al., 1999, 2000a, b; Jones et al., 1999, 2000).

Radiation transfer in the snow pack controls the depth to which photochemical processes occur. The

\*Corresponding author. Tel.: +1-907-474-7235; fax: +1-907-474-5101.

E-mail address: wrs@ozone.gi.alaska.edu (W.R. Simpson).

<sup>1</sup>Present address: Department of Chemistry, King's College London, Strand, London WC2R 2LS, UK.

<sup>2</sup>Also at C.N.R.-Istituto sull'Inquinamento Atmosferico, Rome, Italy.

simplest model for radiative transfer in the snow uses the two-stream approximation. Within this approximation, two diffusely propagating beams, one downwelling, and one upwelling are assumed to describe the radiation within the snow pack. Under conditions where the light is fairly diffuse, this approximation is probably not too severe and may give accurate results. However, in the near-surface layer, where direct sunlight is present, this approximation cannot accurately describe the light field.

Because snow grains are significantly larger than the wavelength of UV and visible light, most light is forward scattered, making the scattering phase function highly asymmetric. The delta-Eddington approximation (Wiscombe, 1977; Wiscombe and Joseph, 1977) has been shown to be fairly accurate for modeling highly asymmetric scattering phase functions, thus we have selected to use it in our modeling of radiation transfer in snow. The delta-Eddington approximation separates the scattering phase function into a forward-scattered peak, modeled by a delta function, and a more diffuse portion, which is modeled by the Eddington approximation.

The delta-Eddington computer code used in this study incorporates both diffuse and direct radiation (Wiscombe, 1977). The diffuse radiation field is described by the Eddington assumption, truncated Legendre expansion, retaining only the two lowest-order terms. Thus, the total radiance field as a function of polar angle  $\theta$  and polar azimuth  $\phi$  is

$$L(\theta, \phi) = F_0 \delta(\theta - \theta_0) \delta(\phi - \phi_0) + L_0 + L_1 \cos \theta, \quad (1)$$

where  $L$  is the total radiance field,  $F_0$  is the direct sun flux,  $\delta$  is the delta function,  $\theta_0$  and  $\phi_0$  are the solar zenith and azimuth angles, respectively, and  $L_0$  and  $L_1$  describe the diffuse field. It is most common to refer to the diffuse field by describing its upwelling and downwelling irradiances. The irradiance is the integral of the radiance field over the upwelling or downwelling hemispheres weighted by the cosine of the incident light angle. Thus, the direct irradiance,  $E_0$ , diffuse downwelling,  $E_{d\downarrow}$ , and diffuse upwelling irradiance,  $E_{d\uparrow}$  are given by

$$\begin{aligned} E_0 &= F_0 \cos \theta_0, \\ E_{d\downarrow} &= \pi L_0 + \frac{2\pi}{3} L_1, \\ E_{d\uparrow} &= \pi L_0 - \frac{2\pi}{3} L_1 \end{aligned} \quad (2)$$

The most commonly observed parameters are the total downwelling irradiance,  $E_{\text{tot}} = E_0 + E_{d\downarrow}$ , the direct to total irradiance ratio,  $r = E_0/E_{\text{tot}}$ , and the albedo,  $A = E_{d\uparrow}/E_{\text{tot}}$ . We observed all these parameters at the ALERT 2000 field site (Simpson et al., 2002), and will use our observations to constrain and test the radiation transfer model, as described later.

One can also calculate the corresponding components of the actinic flux. The direct sun actinic flux is simply

$F_0$ , and the diffuse components of the actinic flux are

$$\begin{aligned} F_{d\downarrow} &= 2\pi L_0 + \pi L_1, \\ F_{d\uparrow} &= 2\pi L_0 - \pi L_1. \end{aligned} \quad (3)$$

The total actinic flux,  $F_{\text{tot}} = F_0 + F_{d\downarrow} + F_{d\uparrow}$  is then independent of the diffuse asymmetry term,  $L_1$ . Our overall goals in this paper are to achieve a qualitative understanding of the total actinic flux within the snow pack as well as a quantitative prediction of actual actinic fluxes within the snow pack based upon measurements of irradiance we made during the ALERT 2000 field campaign.

## 2. Model calculations

We can gain an understanding of the effect of direct to diffuse light conversion based upon simple model calculations. We used the Wiscombe Fortran code for solving the delta-Eddington equations (Wiscombe, 1977). The snow optical properties for our model are the single-scattering albedo,  $\omega$ , and the asymmetry parameter,  $g$ . The single-scattering albedo is the ratio of the scattering optical depth to the total extinction optical depth,  $\omega = \tau_{\text{scat}}/(\tau_{\text{scat}} + \tau_{\text{abs}})$ . As we will see later, an appropriate value for Alert snow in the UV region is  $\omega = 0.99995$ . Mie calculation by Warren for 100  $\mu\text{m}$  radius ice spheres indicate that an appropriate value for the  $g$  factor in the UV is  $g = 0.886$  (Warren, 1982). The values of these optical properties ( $g$  and  $\omega$ ) vary with wavelength, leading to wavelength-dependent penetration of light in snow. For the purpose of these model calculations, we will simply take appropriate values, stated above.

The snow pack is assumed to have a large optical depth so that the albedo of the underlying surface does not affect the calculation. We call this snow pack semi-infinite. In regions where snow persists for much of the winter, the total pack thickness is typically sufficient to be in the semi-infinite limit. In cases where the snow is thinner, the calculation will depend on the albedo of the underlying surface. In the semi-infinite regime, the snow must have some absorption ( $\omega < 1$ ) because purely scattering snow is always sufficiently transmissive to have the underlying albedo affect the calculation. Thus, in the semi-infinite limit, the absorption and scattering cross sections combine to control the optical penetration depth. In this way, typical snow packs are different from clouds, which are sometimes taken as purely scattering at visible and ultraviolet wavelengths (Madronich, 1987).

We selected four solar radiation cases, three with completely direct sun, with solar zenith angles of  $0^\circ$  (case (a)),  $60^\circ$  (case (b)), and  $84^\circ$  (case (c)), and one case with purely diffuse radiation (case (d)). These angles are

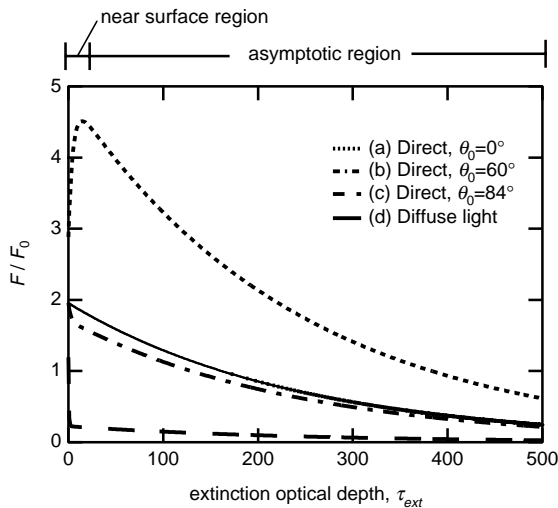


Fig. 1. The ratio of the in-snow actinic flux,  $F(\tau_{\text{ext}})$ , to the incident actinic flux,  $F_0$  as a function of extinction optical depth within the snow pack,  $\tau_{\text{ext}}$ . Four cases of incident light conditions are shown. Cases (a)–(c) have purely direct sun light at three solar zenith angles. In case (a)  $\theta_0 = 0^\circ$ ,  $\mu = 1.0$ ; case (b)  $\theta_0 = 60^\circ$ ,  $\mu = 0.5$ ; and case (c)  $\theta_0 = 84^\circ$ ,  $\mu = 0.1$ . In case (d), all incident light is assumed to be diffuse.

picked to have convenient values of the cosine of the solar zenith angle ( $\mu = \cos \theta_0$ ). Fig. 1 shows the ratio of the in-snow actinic flux,  $F(\tau_{\text{ext}})$ , to the incident downwelling actinic flux,  $F_0$  as a function of extinction optical depth within the snow pack,  $\tau_{\text{ext}}$ . The optical depth is proportional to physical depth within the snow pack for homogeneous snow. Each direct sun case (cases (a)–(c)) shows a shallow near-surface region where the extinction of radiation is non-exponential followed by an asymptotic region, where the extinction of radiation is exponential with depth in the snow pack. The diffuse radiation case, case (d), has no non-exponential region, indicating that the origin of the near-surface behavior is conversion of direct light to diffusely propagating light. All four cases show the same asymptotic behavior, an exponential decrease in actinic flux with depth. The decrease in actinic flux is most easily parameterized by the  $e$ -folding optical depth of this model snow pack, which is the depth over which the actinic flux decreases by a factor of  $e$ . Because the light is diffuse in the asymptotic region, the irradiance and actinic flux are related by a constant ratio, and both the actinic flux and irradiance decrease with the same  $e$ -folding depth.

Typically, the presence of the snow increases the actinic flux within the topmost layers of the snow pack. One origin for this increase is the high albedo of the snow in the UV region. The albedo is nearly one; thus, actinic fluxes are roughly doubled (e.g. case (d)) near the surface. Note that the in-snow actinic flux divided by the

incident downwelling actinic flux is being plotted, and that the presence of the snowpack also increases the actinic flux above the snow. The calculated actinic flux at the snow surface is equal to the actinic flux for the atmosphere above the snow. For the direct sun cases, (a)–(c), the near-surface region can either increase or decrease the actinic flux, dependent on solar zenith angle. For overhead sun, case (a), the actinic flux is significantly enhanced by the conversion of direct light to diffuse light. Madronich (1987) reported the enhancement of the actinic flux inside and above the clouds as compared to the incident actinic flux. Madronich argues that this enhancement is caused by the conversion of direct light to diffusely propagating light in the cloud. Because snow pack converts direct to diffuse light, it achieves a similar flux enhancement. We note that the functional form of the enhancement in semi-infinite snow is different from that in the clouds calculated by Madronich because he assumed that the cloud was conservative ( $\omega = 1$ ), which is never the case for semi-infinite snow. Madronich (1987) argues that the enhancement factor is  $\approx 2 \cos \theta_0$ . The maximum actinic flux enhancement is over four times the incident actinic flux, which occurs very near the snow's surface.

For glancing incidence light, case (c), the actinic flux in the near-surface layer is decreased compared to the other cases. The origin of this effect is the forward scattering of light by snow. When light is incident on snow at a glancing incidence angle, scattering by a small angular deviation can redirect the light back out of the snow pack. Therefore, less of the direct beam is converted to diffuse radiation within the snow pack when light is incident at a glancing angle (high solar zenith angle) than when light is incident at a normal incidence (low solar zenith angle). The complement of this behavior is seen in the snow pack albedo. The reflectivity of snow increases at high solar zenith angles as compared to low solar zenith angles (Warren, 1982).

Our delta-Eddington model assumes the snow pack is plane parallel, while real snow packs have rough surfaces. This surface roughness will make the local angle of incidence of a light ray into snow different from the angle of incidence into a horizontal surface (as the model assumes). Therefore, one would expect that roughness should diminish the solar zenith angle dependence of the reflectivity and conversion of direct to diffuse light within the snow pack. For the purpose of this paper, we will retain the assumption of a flat surface, and simply note that roughness may lead to significant effects.

Our model calculations indicate that semi-infinite snow pack can be divided into two regions, a near-surface region, where conversion of direct to diffuse light occurs, and an asymptotic region, where the light is very diffuse and decreases exponentially with distance in the snow pack. In the near-surface region, the conversion

process depends strongly on the solar zenith angle. In a real situation, the incident light consists of both direct and diffuse light with the fraction of direct light being strongly dependent on sky condition (clouds and Rayleigh or aerosol scattering), solar zenith angle, and wavelength. In general, UV light becomes more diffuse at high solar zenith angles, which minimizes the snow-pack actinic flux decrease seen in model calculation case (c). On the other hand, at low solar zenith angles, the fraction of direct light should remain large, and high actinic flux enhancements, as seen in case (a) are predicted.

### 3. Application of delta-Eddington model to ALERT 2000 data

For 6 weeks during the light-intensive period of the ALERT 2000 campaign, we measured a nearly continuous record of the total downwelling spectral irradiance from 300 to 422 nm (King and Simpson, 2001). At some times, we also measured downwelling irradiance in other spectral windows covering the visible to near IR. We also measured the light intensity at various locations within the snow pack and found the decrease in light intensity with depth to be exponential for homogeneous snow pack in the asymptotic region. In a previous publication (King and Simpson, 2001), we reported the asymptotic  $e$ -folding depths as a function of wavelength for a homogeneous snow pack. This snow pack had a temperature of  $-30^{\circ}\text{C}$ , a density of  $0.25\text{ g cm}^{-3}$ , and a grain radius of about  $100\text{ }\mu\text{m}$  (estimated by hand loupe). More detailed microscope measurements by Domine et al. (personal communication) indicate that the actual morphology of snow was much more complex than our estimates. Because our snow optical properties are based upon a Mie scattering calculation for spheres, we kept our estimate of the effective radius of particles of  $100\text{ }\mu\text{m}$ .

We used the results of Warren's Mie scattering calculation for pure-ice spheres with  $100\text{ }\mu\text{m}$  radius as a basis of our optical properties (Brandt and Warren, 1993; Warren, 1982). These calculations give three results as a function of wavelength;  $Q_{\text{ext}}(\lambda)$ , the extinction efficiency,  $g(\lambda)$ , the asymmetry factor, and  $\omega(\lambda)$ , the single-scattering albedo. The single-scattering co-albedo is  $1 - \omega$ . The extinction optical depth of a layer,  $\Delta\tau_{\text{ext}}$ , of thickness  $\Delta z$  is given by

$$\Delta\tau_{\text{ext}} = \frac{0.75 Q_{\text{ext}}}{r_{\text{grain}}} \frac{\rho}{\rho_{\text{ice}}} \Delta z, \quad (4)$$

where  $\rho$  is the bulk density of the snow, and  $\rho_{\text{ice}}$  is the density of pure ice and  $r_{\text{grain}}$  is grain radius.

Using these optical properties for pure ice, we calculated the downwelling irradiance as a function of depth and wavelength. As discussed in the model

calculation, in the asymptotic region, the decrease with distance is quantified by the  $e$ -folding depth. The  $e$ -folding depth calculated by the pure-ice optical properties is longer than the observed  $e$ -folding depth at all wavelengths. This observation indicates that there is an additional absorber in the snow at Alert. Because the absorption is controlled by the single-scattering co-albedo, we increased the co-albedo until we achieved agreement between observed and modeled in-snow irradiance measurements. Fig. 2 shows the optical properties,  $1 - \omega$ ,  $g$ , and  $Q_{\text{ext}}$ , used to model the snow at Alert. Note that the exact form of the co-albedo depends strongly on the assumed grain radius of the ice spheres, and thus our optical properties are not completely unique. One could alternatively assume that scattering by small-scale features on the snow grains could explain the short length of the  $e$ -folding depth (Gerland et al., 1999). If one assumes that the ice spheres have a smaller effective radius, the co-albedo that is required to make the model agree with irradiance measurements becomes smaller, while an assumption

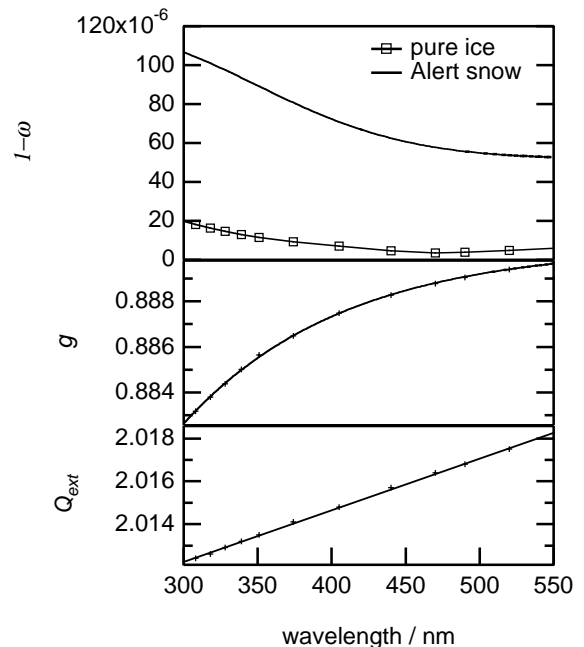


Fig. 2. The optical properties used to model snow at Alert. The co-albedo ( $1 - \omega$ ), asymmetry factor ( $g$ ), and extinction efficiency ( $Q_{\text{ext}}$ ) are shown as a function of wavelength. Two curves are shown for the co-albedo, open box symbols represent the co-albedo for pure water ice, as calculated by the Mie code, and solid lines without symbols represent the co-albedo for Alert snow. The Alert snow co-albedo was determined by assuming that the asymmetry factor and extinction efficiency of the snow is the same as calculated by the  $100\text{ }\mu\text{m}$  radius ice sphere Mie calculation and adjusting the co-albedo until the model reproduced the observed spectral irradiances at depth.

of larger ice spheres requires an increase in co-albedo for the model to agree with irradiance measurements. On the other hand, sensitivity studies indicate that models with either double or half the assumed particle radius (200 or 50  $\mu\text{m}$ , respectively) and appropriate co-albedo to reproduce the irradiance within the snow pack have essentially identical in-snow pack actinic fluxes. Therefore, it is most important to use a consistent set of optical properties for modeling light in snow. The co-albedo (absorption) used in the model is dependent on the assumed snow grain size.

The fraction of direct radiation depends on wavelength, sky condition (cloud, aerosol), and solar zenith angle. We measured direct and diffuse components of the downwelling irradiance over a full clear day by a shadow-masking procedure. This procedure is described in another publication in this issue (Simpson et al., 2002). The measurements were then fit to a function of wavelength and solar zenith angle

$$r = \frac{E_0}{E_{\text{tot}}} = f(\lambda, \theta_0). \quad (5)$$

This functional form was used to set the snow surface boundary condition ratio between  $E_0$  and  $E_{d\downarrow}$  in the model during clear sky conditions. Because the irradiance as a function of depth within the snow pack is directly dependent on the surface downwelling irradiance, we are able to make all calculations with a constant downwelling irradiance spectrum  $E_{\text{tot}}(\lambda) = 1$ , then multiply by the observed downwelling irradiance spectrum at the surface to give the irradiance versus depth within the snow pack. We refer to all calculations with a constant downwelling irradiance spectrum,  $E_{\text{tot}}(\lambda) = 1$ , as normalized calculations (which will be symbolized by putting a bar over the calculated quantity). Thus, the downwelling irradiance as a function of depth is given by

$$E(\lambda, z) = E_{\text{tot}}(\lambda) \bar{E}(\lambda, z), \quad (6)$$

where  $E_{\text{tot}}(\lambda)$  is the observed surface total downwelling irradiance, and  $\bar{E}(\lambda, z)$  is the normalized downwelling irradiance as a function of wavelength and depth. Note that the model calculated,  $\bar{E}(\lambda, z)$ , depends on the direct and diffuse irradiance fractions and solar zenith angle.

Fig. 3 shows the observed and modeled irradiance spectra within the snow pack. The surface irradiance spectrum is used as a boundary condition in the model, and hence no model result is shown for the surface irradiance. It is clear that the model achieves very good agreement with the observed irradiance spectra versus depth. The 8.5 cm observed spectrum appears vertically offset from the modeled spectrum. A vertical offset of 6 mm for this fiber's position would bring the modeled spectrum into agreement with the observed spectrum. We had previously estimated our ability to measure the positions of each fiber optic sensor to be  $\pm 5\text{mm}$ ;

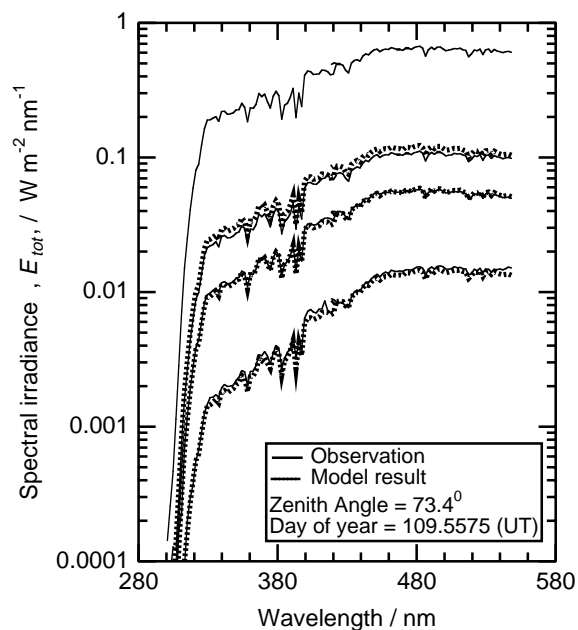


Fig. 3. The observed and modeled spectral irradiance as a function of depth in the snow pack. Because the model takes the surface irradiance spectrum as input, only model results for the three in-snow spectra are shown. The depths of the spectra within snow were 8.5, 12.6, and 20.4 cm. The observed discrepancy for the 8.5 cm spectrum is most likely due to an error in measurement of that fiber's position within the snow pack.

therefore, we feel it likely that the offset of this spectrum is due to improper measurement of the depth of one of the fiber optic sensors. The good agreement of observations with the modeled irradiance spectra versus depth indicates that the model is properly calculating the spectral transmission of Alert snow.

Having tested the irradiance properties of the model, we can now calculate the actinic flux versus depths in the snow pack. We calculated the normalized total actinic flux,  $\bar{F}_{\text{tot}}(\lambda, z)$ , as a function of wavelength and depth within the snow pack at  $2^\circ$  solar zenith angle increments. The normalized actinic flux is the unitless ratio of the actinic flux to the downwelling irradiance incident on the snow pack. We then multiply the normalized actinic flux by the downwelling surface irradiance to get the snow pack actinic flux

$$F_{\text{tot}}(\lambda, z) = E_{\text{tot}}(\lambda) \bar{F}_{\text{tot}}(\lambda, z). \quad (7)$$

During cloudy conditions, as described in Simpson et al. (2002), all incident light on the snow was considered to be diffuse (i.e.  $r = 0$ ). We then calculated the normalized total actinic flux for cloudy sky conditions and used this result during overcast times.

Fig. 4 shows the normalized total actinic flux calculated at a  $66^\circ$  solar zenith angle as a function of

wavelength and depth. Note that there is again a shallow non-exponential layer near the surface (first few millimeters) followed by an exponential decrease with distance in the snow pack. The presence of the non-exponential layer is seen most strongly at the long-wavelength side of the plot.

#### 4. Photolysis of nitrate in snow

Application of the delta-Eddington model to radiation transfer within the Alert snow pack, allows the prediction of the total actinic flux as a function of depth and wavelength within the snow pack. Multiplying the actinic flux by the appropriate absorption cross section and quantum yield and integrating over all wavelengths gives the depth-resolved photolysis rate coefficient

$$J(z, t) = \int F_{\text{tot}}(\lambda, z, t) \sigma(\lambda) \Phi(\lambda) d\lambda. \quad (8)$$

We are interested in photolysis of nitrate ion,  $\text{NO}_3^-$ , in snow to give  $\text{NO}_2$ . Although there are no measurements of the atmospherically relevant absorption cross section of nitrate in snow, measurements of the far UV band (Berland et al., 1996) indicate that the ice environment is similar to aqueous solution. Assuming the ice-adsorbed state is similar to that of aqueous nitrate ion, we can use

the aqueous absorption band of  $\text{NO}_3^-$  (Meyerstein and Treinin, 1961) as a model for ice-adsorbed nitrate ion.

The quantum yield for production of  $\text{NO}_2$  from nitrate photolysis in aqueous solution has been measured (Mark et al., 1996; Zellner et al., 1990; Zepp et al., 1987). Zellner et al. (1990) measured the room temperature (298 K) quantum yield,  $\Phi = 0.017$ , in the 300-nm band, in agreement with the measurement of Zepp et al. (1987). Mark et al. (1996) measured  $\Phi = 0.09$  at 254 nm (between the 200 and 300 nm bands), approximately a factor of five higher, although the different wavelength may be at least partially responsible for the change. Zellner et al. (1990) measured the temperature dependence, which they interpreted as a cage effect. If we extrapolate their measurements to snow temperatures of 243 K, the calculated quantum yield is  $\Phi = 0.0043$ . Of course, in making this extrapolation, we have ignored the phase change from liquid water to ice. If nitrate is concentrated at surfaces in ice, it may be more likely to produce gas-phase  $\text{NO}_2$ , therefore, we see  $\Phi = 0.0043$  as a lower bound with significant possibility of larger quantum yield. If we had taken the Mark et al. (1996) quantum yield, and assumed that it was temperature independent, the quantum yield would be 20 times larger. To be conservative in our calculations, we take Zellner's temperature-dependent form extrapolated to snow temperatures ( $\Phi = 0.0043$  at 243 K).

Fig. 5 shows the calculated photolysis rate of nitrate ion in snow as a function of depth and time. The noon-time lifetime is over 150 days (using  $\Phi = 0.0043$ ), indicating that nitrate in snow is not highly depleted on the month timescale, but over the entire summer

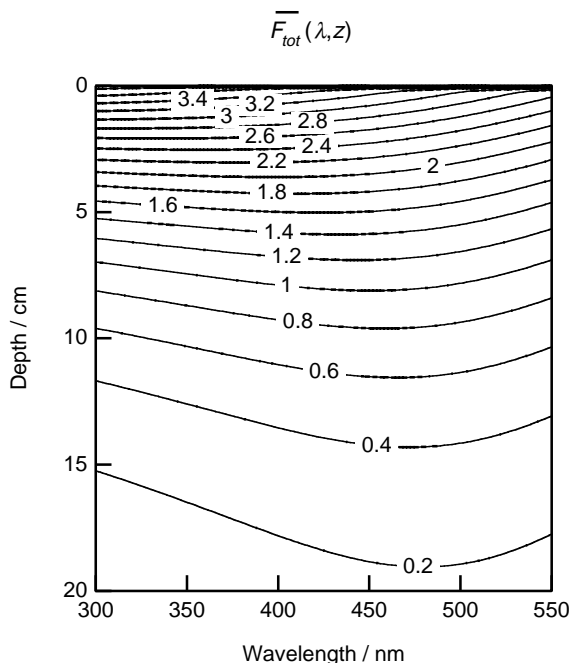


Fig. 4. The normalized total actinic flux,  $\overline{F}_{\text{tot}}(\lambda, z)$ , as a function of wavelength and depth within the snow pack. This calculation uses a solar zenith angle of  $66^\circ$ , which is near the noon solar zenith angle for April in Alert.

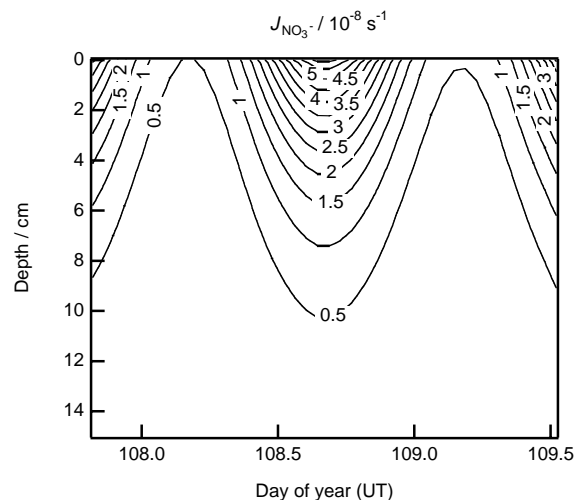


Fig. 5. Calculated photolysis rate of nitrate in snow as a function of depth and time. Contours of the photolysis rate of  $\text{NO}_3^-$  ion are shown versus depth in the snow pack and time (UT). The results shown have been divided by  $10^{-8} \text{ s}^{-1}$ .

(with higher solar elevations and thus higher photolysis rates and shorter lifetime), depletion of  $\text{NO}_3^-$  is likely to be significant. If we were to use the Mark et al. (1996) quantum yield,  $\Phi = 0.09$ , the nitrate lifetime would be only 1 week.

Integrating the photolysis rate over depth within the snow pack gives the total snow pack photolysis rate, which has units of a transfer velocity:

$$V_{\text{NO}_3^-}(t) = \int J(z, t) dz. \quad (9)$$

Fig. 6 shows the maximum transfer velocity as a function of time. The diurnal shape of the maximum transfer velocity is very similar to the flux of  $\text{NO}_x$  and HONO proposed to be produced by snow-pack nitrate photolysis (Zhou et al., 2001; Beine et al., 2002). If we assume that all photo-produced nitrogen oxides are released to the atmosphere, we can multiply the transfer velocity by the concentration (number density) of nitrate in snow,  $N_{\text{NO}_3^-}$ , to calculate the maximal flux of nitrogen oxides from  $\text{NO}_3^-$  photolysis:

$$F_{\text{NO}_x}(t) = V_{\text{NO}_3^-}(t) N_{\text{NO}_3^-}. \quad (10)$$

For typical number densities of  $\text{NO}_3^-$  in Alert snow (6–9  $\mu\text{M}$  liquid concentration, snow density of 0.25  $\text{g}/\text{cm}^3$ ), we can calculate the maximal chemical flux of nitrogen oxides. Assuming snow nitrate concentration is 8  $\mu\text{M}$ , we calculate  $F_{\text{NO}_x} = 1.8 \times 10^{-8} \text{ mol m}^{-2} \text{ h}^{-1}$  on DOY 108 noon.

Beine et al. (2002) report a noon-time flux of  $\text{NO}_x$  of  $3 \times 10^{-8} \text{ mol m}^{-2} \text{ h}^{-1}$ . Zhou et al. (2001) has observed photochemical production of HONO from snow pack and has argued that photo-produced  $\text{NO}_2$  can further react to HONO in the presence of acidic snow. The noon-time flux reported by Zhou et al. (2001) is

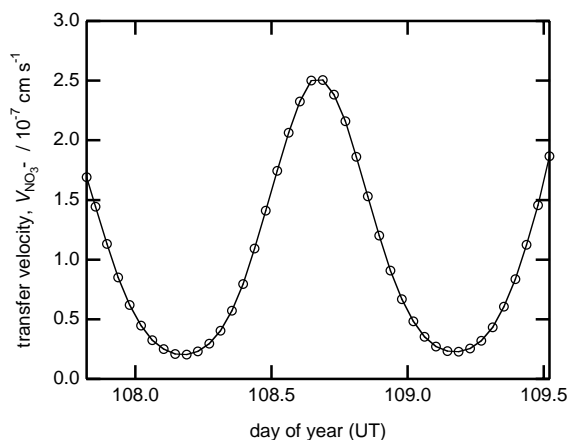


Fig. 6. The maximal transfer velocity for products of nitrate ion photolysis within snow versus time (UT). Multiplying this value by the  $\text{NO}_3^-$  concentration gives the maximal flux of nitrogen oxides produced via snow-pack nitrate photolysis.

$4 \times 10^{-8} \text{ mol m}^{-2} \text{ h}^{-1}$ . If this mechanism is correct and the conversion to HONO is stoichiometric, then the HONO flux should be added to the  $\text{NO}_x$  flux to compare with the calculated maximal flux from snow-pack nitrate photolysis. Thus, the total flux of nitrogen oxides observed is  $7 \times 10^{-8} \text{ mol m}^{-2} \text{ h}^{-1}$ . This value is four times larger than our maximal chemical flux calculated using the temperature-extrapolated Zellner et al. quantum yield. Warmer temperatures that occurred during some of the chemical flux measurements increase our calculated maximal chemical flux by up to 50% over the DOY 108 noon values, coming closer to the observed chemical flux. Alternatively, if the extrapolation to ice temperatures is incorrect, and the quantum yield is higher than predicted from the Zellner et al. (1990) formula, the calculated flux could match or even exceed the observed flux. As an extreme limit, if we use the Mark et al. (1996) quantum yield without temperature correction, the calculated maximal chemical flux would be five times the observed  $\text{NO}_x + \text{HONO}$  flux.

## 5. Conclusions

Application of the delta-Eddington radiation transfer model to snow-pack photochemistry allows us to understand photolysis within snow. Simple model calculations show that the actinic flux within the snow pack is enhanced by multiple scattering. The scattering and absorption properties of the snow as well as the solar zenith angle and fraction of direct to diffuse radiation incident on the snow pack control the depth to which radiation penetrates snow and the relationship between the actinic flux and irradiance. The radiation transport is characterized by two regimes, a near-surface region, where direct light is converted to diffuse light, and an asymptotic region, where light decreases exponentially with distance. In the case of shallow snow packs, a third region also occurs, where the albedo of the surface below the snow pack affects the radiation transfer.

We use this model to convert observations of spectral irradiance as a function of depth to spectral actinic fluxes, which can then be multiplied by absorption spectra and quantum yields to result in photolysis rates. Using the assumption that the absorption spectrum and quantum yield of nitrate anion ( $\text{NO}_3^-$ ) in snow are the same as in aqueous solution (extrapolated to  $-30^\circ\text{C}$ ), we calculate a photolysis rate coefficient for nitrate in snow. Assuming all of the  $\text{NO}_2$  produced by this process is released to the atmosphere, we derive a maximal flux of nitrogen oxides from nitrate photolysis. Under acidic conditions, this  $\text{NO}_2$  can be converted to HONO. The diurnal shape of the nitrate transfer velocity curve is very similar to the flux of HONO produced from the snow pack, as observed by Zhou et al. (2001), as well as

being similar to the  $\text{NO}_x$  flux observed by Beine et al. (2002). The noon-time maximal flux predicted by this calculation using a lower bound for the quantum yield is  $\approx 4$  times less than the observed  $\text{HONO} + \text{NO}_x$  flux. When other photochemical mechanisms are proposed, this model can be used to calculate photo-produced fluxes from the snow pack. The lack of absorption spectra and quantum yields for snow-pack photochemical processes and independent confirmation of the model-predicted photolysis rates are obstacles that need to be surmounted to apply this method with confidence in the general case.

### Acknowledgements

Martin King and William Simpson wish to thank the Frontier Research System for Global Change for financial support of this project. Martin King wishes to thank Frontier Research System for Global Change for postdoctoral support. We also thank Alan Gallant, Jan Bottenheim, and Paul Shepson without whose help and support during the Polar Sunrise Experiment ALERT 2000 campaign, these measurements would not have been possible.

### References

- Beine, H.J., Honrath, R.E., Domini, F., Simpson, W.R., Fuentes, J.D., 2002.  $\text{NO}_x$  during background and ozone depletion periods at Alert: fluxes above the snow surface. Submitted to JGR.
- Berland, B.S., Foster, K.L., Tolbert, M.A., George, S.M., 1996. UV absorption spectra of  $\text{H}_2\text{O}/\text{HNO}_3$  films. *Geophysical Research Letters* 23 (20), 2757–2760.
- Brandt, R.E., Warren, S.G., 1993. Solar-heating rates and temperature profiles in Antarctic snow and ice. *Journal of Glaciology* 39 (131), 99–110.
- Couch, T.L., Sumner, A.L., Dassau, T.M., Shepson, P.B., Honrath, R.E., 2000. An investigation of the interaction of carbonyl compounds with the snowpack. *Geophysical Research Letters* 27, 2241–2244.
- Gerland, S., Winther, J.G., Orbaek, J.B., Liston, G.E., Oritsland, N.A., Blanco, A., Ivanov, B., 1999. Physical and optical properties of snow covering Arctic tundra on Svalbard. *Hydrological Processes* 13 (14–15), 2331–2343.
- Hoffman, M.R., 1996. Possible chemical transformations in snow and ice induced by solar (UV photons) and cosmic irradiation (muons). In: Wolff, E.W., Bales, R.C. (Eds.), *Chemical Exchange Between the Atmosphere and Polar Snow*. Springer, New York, pp. 353–377.
- Honrath, R.E., Peterson, M.C., Guo, S., Dibb, J.E., Shepson, P.B., Campbell, B., 1999. Evidence of  $\text{NO}_x$  production within or upon ice particles in the Greenland snowpack. *Geophysical Research Letters* 26 (6), 695–698.
- Honrath, R.E., Guo, S., Peterson, M.C., Dziobak, M.P., Dibb, J., Arsenaault, M.A., 2000a. Photochemical production of gas-phase  $\text{NO}_x$  from ice-crystal  $\text{NO}_3^-$ . *Journal of Geophysical Research* 105, 183–190.
- Honrath, R.E., Peterson, M.C., Dziobak, M.P., Dibb, J.E., Arsenaault, M.A., Green, S.A., 2000b. Release of  $\text{NO}_x$  from sunlight-irradiated midlatitude snow. *Geophysical Research Letters* 27 (15), 2237–2240.
- Hutterli, M.A., Roethlisberger, R., Bales, R.C., 1999. Atmosphere-to-snow-to-firn transfer studies of HCHO at Summit, Greenland. *Geophysical Research Letters* 26 (12), 1691–1694.
- Jones, A.E., Weller, R., Minikin, A., Wolff, E.W., Sturges, W.T., McIntyre, H.P., Leonard, S.R., Schrems, O., Bauguitte, S., 1999. Oxidized nitrogen chemistry and speciation in the Antarctic troposphere. *Journal of Geophysical Research* 104 (D17), 21355–21366.
- Jones, A.E., Weller, R., Wolff, E.W., Jacobi, H.-W., 2000. Speciation and rate of photochemical NO and  $\text{NO}_2$  production in Antarctic snow. *Geophysical Research Letters* 27 (3), 345–348.
- King, M.D., Simpson, W.R., 2001. Extinction of UV radiation in Arctic snow at Alert, Canada (82°N). *Journal of Geophysical Research* 106 (D12), 12499–12508.
- Madronich, S., 1987. Photodissociation in the atmosphere I. Actinic flux and the effects of ground reflections and clouds. *Journal of Geophysical Research* 92 (D8), 9740–9752.
- Mark, G., Korth, H.-G., Schuchmann, H.-P., Von Sonntag, C., 1996. The photochemistry of aqueous nitrate ion revisited. *Journal of Photochemistry and Photobiology A* 101, 89–103.
- Meyerstein, D., Treinin, A., 1961. Absorption spectra of  $\text{NO}_3^-$  in solution. *Journal of Chemical Society, Transactions of Faraday Society* 57, 2104–2112.
- Simpson, W.R., King, M.D., Beine, H.J., Honrath, R.E., Peterson, M.C., 2002. Atmospheric photolysis rate coefficients during the Polar Sunrise Experiment ALERT2000. *Atmospheric Environment* 36, 2471–2480.
- Sumner, A.L., Shepson, P.B., 1999. Snowpack production of formaldehyde and its effect on the Arctic troposphere. *Nature* 398, 230–233.
- Warren, S., 1982. Optical properties of snow. *Review of Geophysical Space Physics* 20, 67–89.
- Wiscombe, W.J., 1977. The delta-Eddington approximation for a vertically inhomogeneous atmosphere. *NCAR Technical Note, NCAR/TN-121 + STR: 1-66*.
- Wiscombe, W.J., Joseph, J.H., 1977. The range of validity of the Eddington approximation. *Icarus* 32, 362–377.
- Zellner, R., Exner, M., Hermann, H., 1990. Absolute OH quantum yields in the laser photolysis of nitrate, nitrite, and dissolved  $\text{H}_2\text{O}_2$  at 308 and 351 nm in the temperature range 278–353 K. *Journal of Atmospheric Chemistry* 10, 411–425.
- Zepp, R.G., Hoigne, J., Bader, H., 1987. Nitrate-induced photooxidation of trace organic chemicals in water. *Environmental Science Technology* 21, 443–450.
- Zhou, X., Beine, H.J., Honrath, R.E., Fuentes, J.D., Simpson, W.R., Shepson, P.B., Bottenheim, J.W., 2001. Snowpack photochemical production of HONO: a major source of OH in the Arctic boundary layer in spring time. *Geophysical Research Letters* 28 (21), 4087–4090.